Economic Geology, v. 118, no. 5, pp. 1219–1229

IN SITU U-Pb DATING OF GARNET AND CASSITERITE FROM THE KANBAUK W-Sn(-F) SKARN DEPOSIT, DAWEI REGION, SOUTHERN MYANMAR: NEW INSIGHTS ON THE REGIONAL Sn-W METALLOGENY IN THE SOUTHEAST ASIAN TIN BELT

Wen Winston Zhao,[1] Mei-Fu Zhou,[1,2,†] and Steven Dudka[3]

[1]*School of Earth Resources, China University of Geosciences, Wuhan, Hubei 430074, China*

[2]*State Key Laboratory of Ore Deposit Geochemistry, Institute of Geochemistry, Chinese Academy of Sciences, Guiyang 550081, China*

[3]*Savitar Exploration Limited, Robinson Road, #20-03 Robinson Point, Singapore 068906*

Abstract

Skarn ores have recently been identified beneath the historically mined placer Sn deposit at Kanbauk of the Dawei region, southern Myanmar. A large-tonnage skarn ore reserve at Kanbauk is estimated to be over 100 million tonnes, with reported ore grades of 0.17% WO_3, 0.26% Sn, and 15.4% CaF_2, potentially making it one of the largest W-Sn skarn deposits in the Southeast Asian tin belt. The mineralized skarns lie between marbles to the east and metasediments of the Mergui Group to the west. The timing of the mineralization is unclear, and thus the genetic relationship with regional magmatic events is not known. We report laser ablation-inductively coupled plasma-mass spectrometry U-Pb ages of garnet and cassiterite from the mineralized skarns. Garnet grains from the massive prograde skarns are typically subhedral to euhedral and show both sector and oscillatory zoning. They have 15 to 23% andradite (Ad), 55 to 67% grossularite (Gr), and 16 to 30% pyralspite (Py) ($Ad_{15\text{-}23}Gr_{55\text{-}67}Py_{16\text{-}30}$) and contain 0.08 to 306 ppm U with a lower intercept $^{206}Pb/^{238}U$ age of 56.0 ± 1.5 Ma. Cassiterite grains from retrograde veinlets are subhedral to anhedral and have U contents from 110 to 12,000 ppm with a lower intercept $^{206}Pb/^{238}U$ age of 54.2 ± 1.7 Ma. Garnet and cassiterite have ages consistent within error and can be taken to indicate the formation of the Kanbauk W-Sn(-F) skarn deposit at around 55 Ma. Together with published ages of primary Sn-W deposits in the Dawei region, our study confirms a westwardly younging trend of mineralization toward the coast and provides support for rollback of the Neo-Tethyan subducting slab since the Late Cretaceous, which is considered as the main mechanism for the regional, extensive Sn-W mineralization.

Introduction

The Southeast Asian tin belt is a north-south elongate zone 2,800 km long and 400 km wide, extending from Yunnan (Southwest China) through Myanmar and Thailand to the Malay Peninsula and Belitung Island in Indonesia (Fig. 1A). Total production has been estimated at 9.6 million tonnes (Mt) of tin, equivalent to 54% of the world's tin production, mostly from eluvial and alluvial deposits in Main Range Malaysia (Schwartz et al., 1995; Lehmann, 2021). Primary production includes a number of quartz-vein- and greisen-type Sn-W deposits, such as the giant Mawchi and Hermyingyi deposits in Myanmar and the Kelapa Kampit and Batu Besi Sn-rich skarns on Belitung Island (Schwartz and Askury, 1990; Gardiner et al., 2016). The recently identified Kanbauk skarn-type W-Sn(-F) deposit lies beneath the historically mined placer Sn mineralization in Kanbauk, Dawei region, southern Myanmar, and exploration up to early 2020 and an unpublished report indicate it to be one of the largest W-Sn skarn deposits in the Southeast Asian tin belt, with estimated skarn ore reserves of over 100 Mt and indicated grades of 0.17% WO_3, 0.26% Sn, and 15.4% CaF_2. Kanbauk skarns identified to date do not show clear association with granitic intrusions; thus, the timing of the mineralization is unclear and the genetic relationship with regional magmatic events poorly understood.

†Corresponding author: e-mail, zhoumeifu@hotmail.com

Garnet and cassiterite contain variable U contents, have high closure temperatures for the U-Pb isotope system (Mezger et al., 1989; Gulson and Jones, 1992), and have been used to directly date skarn ore deposits (e.g., Yuan et al., 2011; Deng et al., 2017; Seman et al., 2017). In this paper, we report the first in situ U-Pb ages of garnet and cassiterite from skarns of the Kanbauk W-Sn(-F) deposit. The U-Pb ages of the two minerals are indistinguishable and coincide well with the field relationships and other published geochronological results for the Sn-W mineralization in the Southeast Asian tin belt. To our knowledge, our work provides the first precise constraints on the timing of the skarn-type W-Sn mineralization in this belt and further provides support for a linkage between the Late Cretaceous to early Eocene regional Sn-W mineralization and the subduction of the Neo-Tethys in Southeast Asia.

Geologic Setting

Southeast Asia witnessed the closure of successive Tethyan oceans and back-arc basins, forming extensive granitoids (Mitchell, 1977; Hutchison and Taylor, 1978; Cobbing et al., 1986; Metcalfe, 2002; Searle et al., 2012; Zaw et al., 2014). The Southeast Asian tin belt comprises mainly three granitoid provinces (Fig. 1A) (Mitchell, 1977, 2018; Searle et al., 2016). The Eastern granitoid province consists predominantly of I-type granites with ages from 289 to 220 Ma, related to the eastward subduction of the Paleo-Tethys (Mitchell, 1977, 2018; Ng et al., 2015). In the Main Range granitoid province, predominantly S-type granites have ages ranging from 227 to

ISSN 0361-0128; doi:10.5382/econgeo.5002; 11 p.

Submitted: February 9, 2022 / Accepted: November 8, 2022

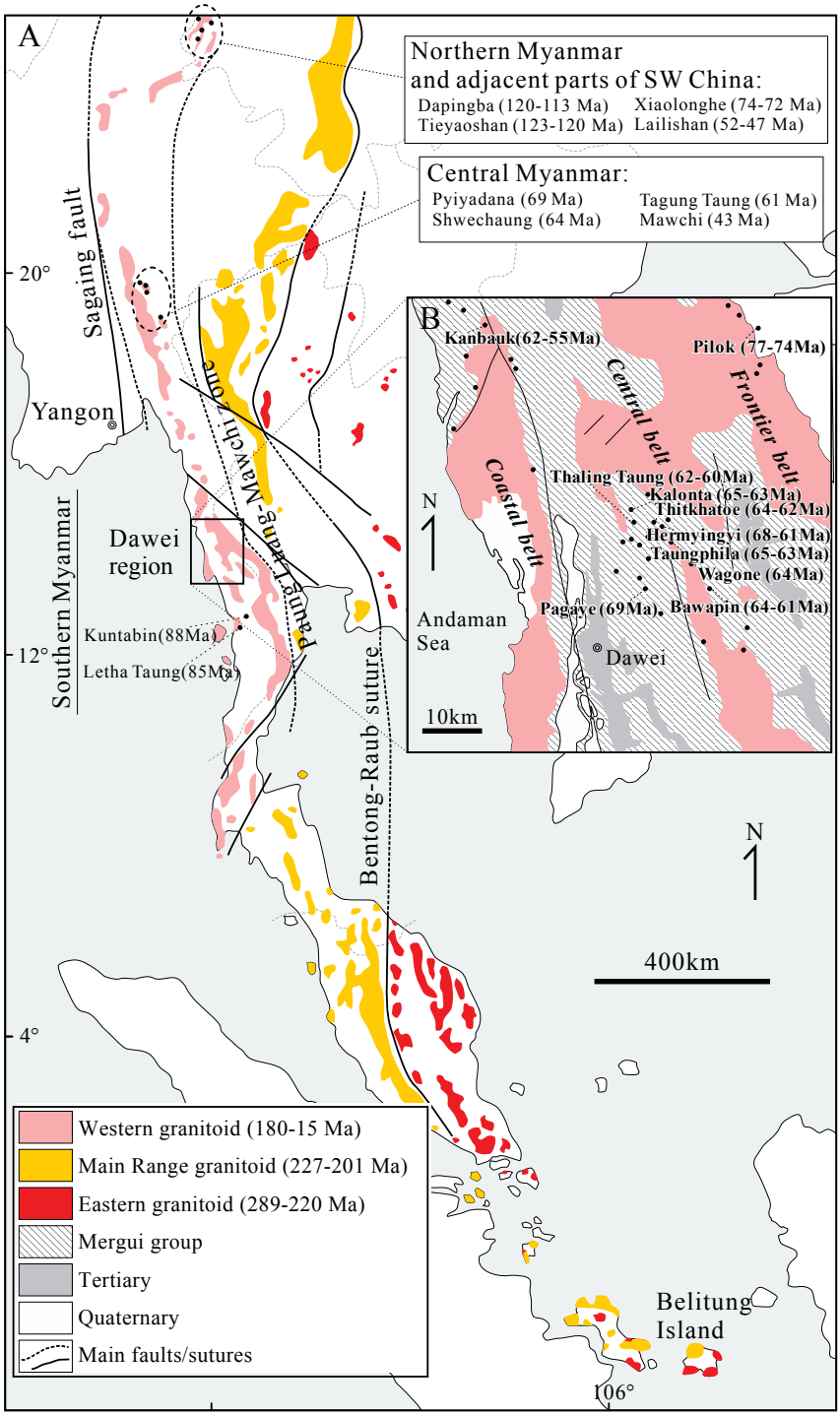

Fig. 1. A: Simplified geologic map of the Southeast Asian tin belt, showing the distribution of granites and W-Sn deposits (modified after Cobbing et al., 1986; Searle et al., 2016). B: Simplified geologic map of the Dawei region, southern Myanmar (modified after Lehmann et al., 1994; Jiang et al., 2017; Myint et al., 2021).

201 Ma and formed in a postcollisional setting after the closure of the Paleo-Tethys (Mitchell, 1977, 2018; Hutchison and Taylor, 1978; Liu et al., 2020; Yang et al., 2020). The Western granitoid province, with a mixture of I-, A-, and S-type granites of mainly Cretaceous to Cenozoic ages, was related to the subduction and closure of Meso- and Neo-Tethys (Mitchell et al., 2012; Crow and Zaw, 2017; Jiang et al., 2017). Both Sn and W deposits occur in the Western granitoid province and are distinct from the Sn-dominant deposits in the Main Range and Eastern granitoid provinces (Mitchell, 2018).

The largest part of the Western granitoid province of the Southeast Asian tin belt is in Myanmar. The Western granitoid province is composed of three granite belts in the Dawei region of southern Myanmar, namely the Coastal,

Central, and Frontier belts from the west to the east (Fig. 1B) (Clegg, 1994). The granites form NNW-SSE–trending elongated bodies in a structural zone parallel to the regional strike of the Mergui Group, which was also called the Slate belt in Myanmar (Mitchell et al., 2012). The Mergui Group is an upper Carboniferous to lower Permian succession composed of a thick sequence of slaty mudstone and pebbly wacke with subordinate limestones and quartzites, and the occurrence of diamictites with cool-water fossils indicates a glacio-marine rift-related depositional environment on the margin of Gondwana (Stauffer and Lee, 1986; Ridd and Watkinson, 2013). Primary mineralization at Hermyingyi, Wagone, Bawapin, Pagaye, Pulatto, and Kalonta and fossil tin placer deposits at Heinda are located in the Central belt (Mitchell, 2018). The Sn-W mineralization is mostly hosted in biotite and two-mica granites (Clegg, 1994). The Coastal belt is mainly built up of biotite granites with minor amounts of hornblende-bearing granodiorite. In the northeastern part of the Coastal belt, there are medium- to coarse-grained aplogranites, the Kanbauk W-Sn(-F) deposit, and other small prospects. In the Frontier belt, several W-Sn deposits are distributed along the border between Myanmar and Thailand, including the Pilok deposit, where the W-Sn mineralization is mainly hosted in the alkali-feldspar aplite granite (Lehmann et al., 1994).

Kanbauk W-Sn Deposit

The Kanbauk deposit (14°35'02"N, 98°01'20"E) is located in the Heinze Chaung channel (Fig. 2A). The commencement of mining activities in the Kanbauk area was by the British-controlled Messrs Redcliff Company in 1916, and it was primarily developed as an alluvial tin mining area. Subordinate tin-tungsten–bearing quartz veins cut the metasediments of the Mergui Group in the west of the mine site, so small-scale hard-rock production also occurred from quartz veins up to the end of World War I. Although the skarn cropped out and was shown on maps in the reports by Griffiths (1917) and Coggin Brown and Heron (1923), it was described as "blue rock" or "basic rock," as skarns had not yet been termed as such or described. The potential economic significance of cassiterite, scheelite, and fluorite in these skarns in the Kanbauk area was not addressed until Savitar's initial evaluation of the project in 2016.

In the Kanbauk area, granites are mainly exposed to the south and west of the mine site. Studies of the igneous rocks in this area are few; however, at least two types of granites are indicated by preliminary reconnaissance mapping: coarse-grained biotite granite and subordinate fine-grained muscovite granite. Currently, it is not clear whether these granites are the causative intrusions or the Kanbauk skarns are related to unexposed granites. The Mergui Group in Kanbauk is expressed as variably hornfelsed siltstones and impure sandstones, generally with shallow dips of about 40° to the west. The rocks of the Mergui Group are usually strongly altered with quartz and skarn veins. A major NW-trending fault controls the NW-SE–trending Heinze Chaung channel, which is subparallel to the regional structure. Limestone was identified during mineral exploration in the Heinze Chaung channel

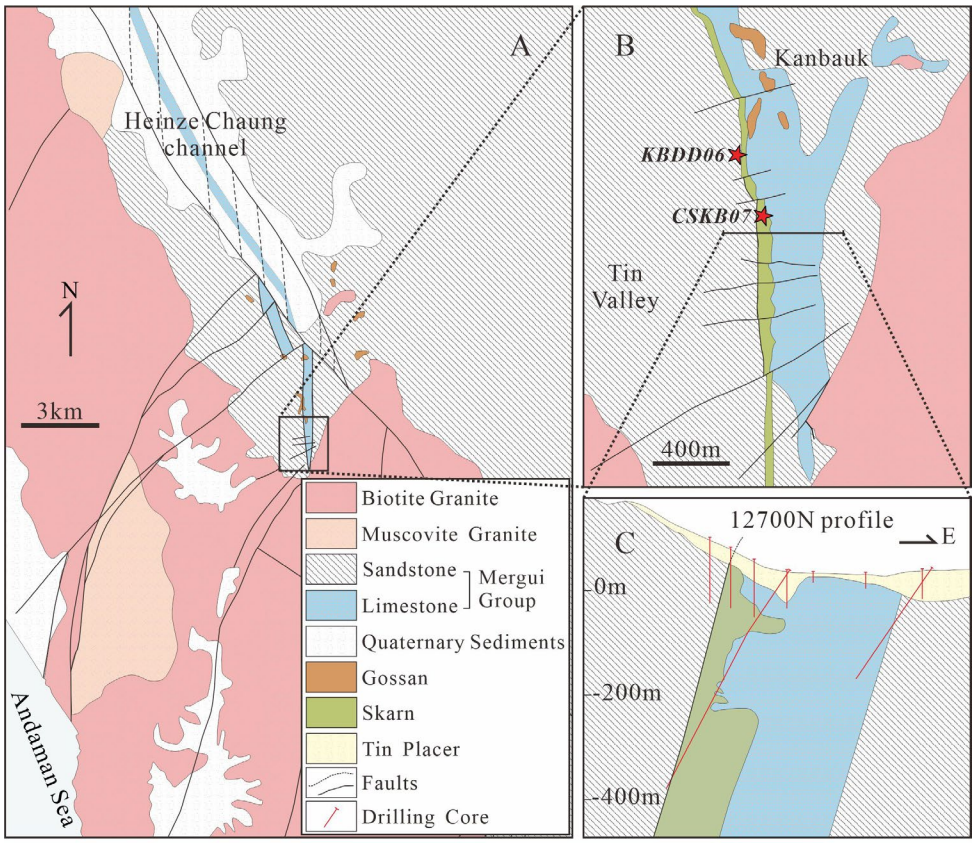

Fig. 2. Simplified geologic map of the Kanbauk deposit, southern Myanmar.

and is covered by Quaternary sediments. Based on historical work, limestone extends for over a distance of at least 16 km along the NW-trending Heinze Chaung channel and south of the Kanbauk mining district (Fig. 2B). This carbonate unit may be part of the Mergui Group but is also considered to be correlated with the middle Permian limestone in Moulmein, about 150 km north of Kanbauk, where it lies unconformably above the Mergui Group (Mitchell, 2018).

The Kanbauk skarns, covered by tin placers on the surface, occur to the west of marbles and to the east in fault contact with the metasediments of the Mergui Group (Fig. 2C). The contact dips steeply to the west at 70° to 80° with projected surface thicknesses ranging between 40 and 80 m. However, some drill cores show interbedding of skarn-altered marble and impure calc-silicate hornfels, and skarn veins extend into the metasediments with late fluorite and scheelite. The eastern contact is irregular and poorly defined. The adjacent marble is cut by veins with skarn minerals and carbonate fluid-escape veins in multiple crosscutting orientations. Gossan occurs on the surface mostly in the north of the mining area, which is considered to be the oxidized distal sulfide skarns. A set of NE-trending faults cut off or displace the southern end of Kanbauk skarns. Locally, the west-northwest to east-southeast faults and fractures are dominant, and quartz veins with wolframite and cassiterite may be related to these structures, but currently it still lacks clear geologic evidence for such a correlation.

Preliminary studies of mineralogy show a prograde skarn stage with massive anhydrous mineral assemblages, including mainly garnet and pyroxene, and a retrograde skarn stage with hydrous and sulfide mineral assemblages either overprinting or forming veinlets cutting prograde assemblages. On a deposit scale, the prograde skarns generally show a typical zonation from red to green garnet to pyroxene outward toward the contact with marble. Wollastonite-pyroxene-vesuvianite assemblages are adjacent to massive garnet skarns. Toward the western contact with metasediments, there is greater predominance of pyroxene skarns with bands of garnet-pyroxene skarns. Scheelite is essentially ubiquitous in both the prograde and retrograde skarns, but the retrograde assemblages have the highest W and Sn grades. Magnetite-rich skarns with wrigglite texture occur locally, typically with abundant fluorite and disseminated scheelite, and may overprint garnet but predate retrograde assemblages. During the retrograde process, garnet skarns were overprinted by assemblages of epidote and carbonate, and pyroxene skarns were overprinted by dark-green actinolite. Cassiterite occurs in late retrograde stages and is associated with carbonate veins and amphibole-chlorite alteration. Sphalerite, galena, pyrrhotite, chalcopyrite, and molybdenite occur in retrograde skarns and associated veins. Some quartz veins contain cassiterite and wolframite in the hornfelsed metasediments of the Mergui Group in Tin Valley, west of the mine site, but no clear crosscutting relationships with skarns are observed.

Sampling and Analytical Methods

Samples for this study were collected from the drill core and outcrop, KBDD06 and CSKB07 (Fig. 2B), in the Kanbauk mine site. Thin sections were made by Savitar in 2017 as part of the earlier petrological studies. Garnet and cassiterite in thin sections were further examined optically to observe their internal textures as well as the occurrence of fluid and mineral inclusions, and preanalyses of their U concentrations. Garnet in sample KB04 and cassiterite in sample KB30 were selected for dating because they contain detectable U and have large enough grain sizes. In sample KB04, garnet grains are coarse and mostly euhedral with both sector and oscillatory zoning, poikilitically enclosing fluorite and pyroxene (Fig. 3A-D). In sample KB30, ghosted concentric zones within prograde metasomatic garnet grains are defined by the distribution of retrograde minerals, and cassiterite grains occur mostly as subhedral to euhedral individual grains or aggregates in veinlets that crosscut early assemblages (Fig. 3E-H).

Major elemental compositions of garnet in massive skarns and cassiterite in crosscutting veinlets were analyzed by JEOL JXA-8230 SuperProbe electron microprobe at the Department of Earth Sciences, The University of Hong Kong. Operating conditions include an acceleration voltage of 15 kV, a beam current of 20 nA, a beam diameter of 5 μm, and a counting time of 30 s. Natural minerals and synthetic glasses from Astimex Standards were used as standards. Analytical results are listed in Table 1.

Garnet grains in the sample KB04 were ablated using a GeoLasPro 193-nm ArF excimer laser (CompexPro 102F, Coherent) coupled to a Thermo Scientific Element XR sector field inductively coupled plasma-mass spectrometry (ICP-MS) instrument at the State Key Laboratory of Ore Deposit Geochemistry, Institute of Geochemistry, Chinese Academy of Sciences, Guiyang. Instrument conditions are listed in Tang et al. (2021) and references therein. Laser beam diameter, fluencies, and repetition rates are 32 μm, 3 J/cm^2, and 5 Hz, respectively. Each analysis consists of 20 s of background acquisition followed by approximately 30 s of sample ablation. Five to eight pulses of preablation were performed in each analysis. Zircon 91500 was used as primary standard material, and garnet Willsboro was used as the secondary standard for monitoring the precision and accuracy of the U-Pb dating results. Cassiterite grains in the sample KB30 were analyzed using an Agilent 7900 ICP-MS instrument equipped with a DUV 193-nm ArF-excimer laser (Geolas 2005, MicroLas Göttingen, Germany) at the State Key Laboratory of Geological Processes and Mineral Resources, China University of Geosciences, Wuhan. All analyses were performed with a laser spot size of 32 μm, a repetition rate of 5 Hz, and a fluence of 8 J/cm^2. Helium was used as the carrier gas in the ablation cell and merged with argon (makeup gas) behind the ablation cell (Luo et al., 2018a). A signal-smoothing and mercury-removing device was used in this laser ablation system to obtain smooth signals and reduce the mercury signal (Hu et al., 2014). Small amounts of water vapor were added to the cell to improve the analytical accuracy and precision (Luo et al., 2018b). Each single-spot analysis consisted of 20 s of background signal acquisition followed by 50 s of ablation. Zircon GJ-1 was used as an external standard to correct the Pb/U fractionation and instrumental mass discrimination; cassiterite AY-4 was analyzed as an unknown. The data collected from ICP-MS of both laboratories were processed offline using the ICPMSDataCal software for calibration, background correction, and floating of integration signal (Liu et al., 2010). Spots that were not contaminated by mineral and fluid inclu-

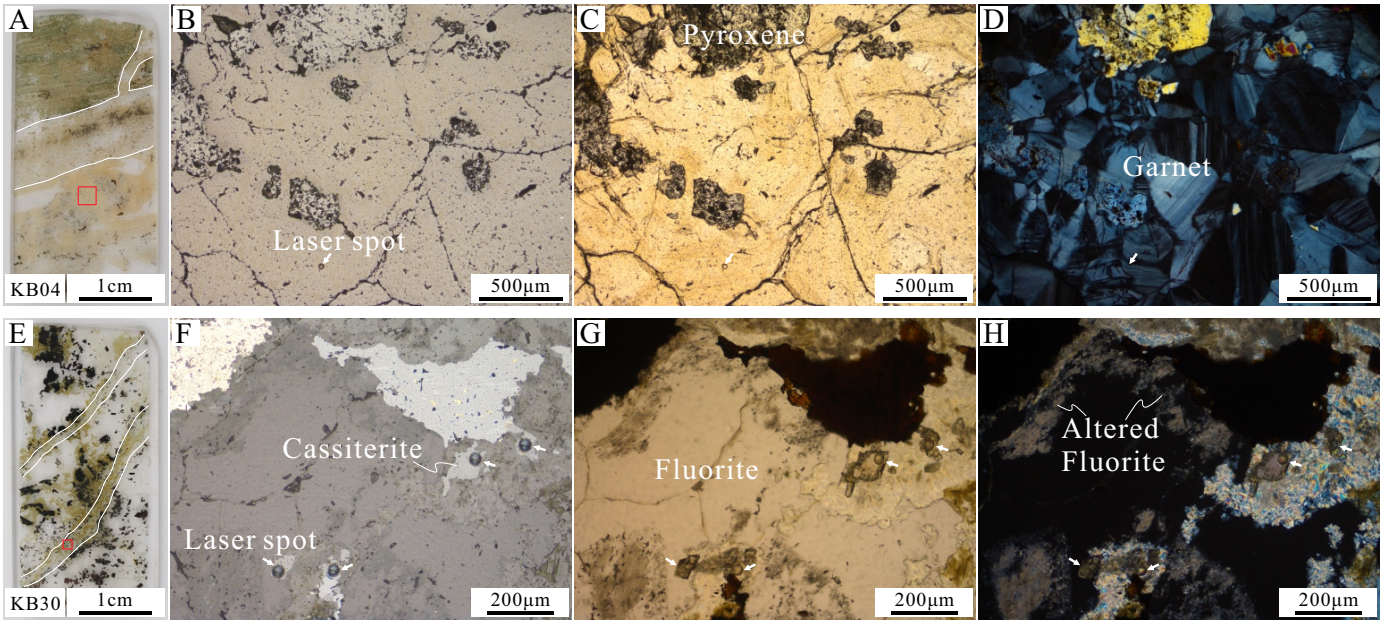

Fig. 3. A: Photomicrograph of sample KB04. The white dashed lines mark the boundaries of pyroxene-garnet, garnet-fluorite, and massive garnet assemblages. The red square outlines the microscopic area in B-D. B: Under reflected light. C: Under plane-polarized light. D: Under cross-polarized light. E: Thin section photo of sample KB30. The white dashed lines mark the cassiterite-bearing veinlets. The red square outlines the microscopic area in F-H. F: Under reflected light. G: Under plane-polarized light. H: Under cross-polarized light.

sions were used for further age calculations. The IsoplotR program was used to calculate U-Pb ages and finish the Tera-Wasserburg concordia to obtain the lower intercept ages (Vermeesch, 2018). The obtained weighted average $^{206}Pb/^{238}U$ age of Willsboro garnet is 1024 ± 14 Ma in this study, consistent with the reference age of 1022 ± 16 Ma (Seman et al., 2017). The obtained weighted average $^{206}Pb/^{238}U$ age of AY-4 garnet is 158.8 ± 3.4 Ma in this study, consistent with the reference age of 158.2 ± 0.4 Ma (Yuan et al., 2011). Analytical results are listed in Table 2.

Analytical Results

Garnet grains from the Kanbauk skarns have a wide range of compositions: 7 to ~49% andradite (Ad), 35 to ~68% grossularite (Gr), and 13 to ~59% pyralspite (Py), all typical of W skarns (Meinert, 1992). Usually, garnet in the prograde skarns is closely related to scheelite, and the electron microprobe analysis results show that those garnet grains contain considerable SnO contents ranging from 0.15 to 0.51 wt % (Table 1). In the retrograde skarns, garnet grains were generally replaced by hydrous and sulfide minerals sometimes with tiny cassiterite grains, implying that Sn was liberated from the garnet structure during the skarn-destructive stages. Different types of veinlets containing scheelite, cassiterite, molybdenite, sphalerite, galena, and pyrrhotite crosscut those early skarn assemblages, representing late-stage mineralization, which may be slightly younger or contemporaneous with the retrograde stage.

Garnet grains used for in situ U-Pb dating have compositions of $Ad_{15–23}Gr_{55–67}Py_{16–30}$, mostly overlapping the typical W and Sn skarns in the ternary diagram (Meinert, 1992). The U contents of garnet grains range from 0.08 to 306 ppm and are suitable for dating. A lower intercept age of 56.0 ± 1.5 Ma (2σ; mean square of weighted deviates [MSWD] = 1.2; n = 26) in the Tera-Wasserburg concordia was obtained (Fig. 4A). Cassiterite grains from veinlets in Kanbauk skarns are generally homogeneous in compositions, with minor amounts of CaO, FeO, MgO, and Nb_2O_5. The U contents of cassiterite grains range from 110 to 12,000 ppm and are also suitable for dating. A lower intercept age of 54.2 ± 1.7 Ma (2σ; MSWD = 4.1; n = 27) in the Tera-Wasserburg concordia was obtained (Fig. 4B). These two ages are apparently consistent within errors, together indicative of the formation of the Kanbauk W-Sn(-F) skarns at around 55 Ma.

In the Kanbauk area, for the subordinate quartz-vein-type cassiterite-wolframite mineralization in the west of the mine site, Zhang et al. (2022) acquired a cassiterite U-Pb age of 61.3 ± 0.6 Ma and a wolframite U-Pb age of 62.4 ± 2.4 Ma, which are both significantly older than the age of the Kanbauk mineralized skarns. These historically mined quartz veins do not show clear relationships with the mineralized skarns, because the west boundary between skarn and metasediments is faulted. Also, the causative granites for both mineralizations remain unknown. Therefore, the only interpretation at this stage is that there might be separate Sn-W mineralizing events in the Kanbauk area. The several-million-year age gaps are also expressed in other deposits. For example, in the Hermyingyi deposit of the Central belt, Jiang et al. (2019) reported a molybdenite Re-Os age of 68.4 ± 2.5 Ma and Zhang et al. (2022) reported cassiterite and wolframite U-Pb ages of 61.6 ± 0.8 and 60.9 ± 1.3 Ma for the potential two-stage quartz-vein-type wolframite-cassiterite mineralizations, which were interpreted to result from the potential two-stage magmatism as recorded by zircon U-Pb ages of 70.0 ± 0.4 and 61.7 ± 1.3

Table 1. Representative Major Elemental Contents of Garnet and Cassiterite from the Kanbauk Skarns, Dawei Region, Southern Myanmar

Garnet	TiO_2 (wt %)	CaO (wt %)	Fe_2O_3 (wt %)	FeO (wt %)	SiO_2 (wt %)	Al_2O_3 (wt %)	SnO_2 (wt %)	MnO (wt %)	P_2O_5 (wt %)	MgO (wt %)	F (wt %)	Total (wt %)	Andradite (%)	Grossularite (%)	Pyralspite (%)
KB02-1	0.02	26.45	3.27	3.70	36.51	19.25	0.37	8.32	0.05	-	0.95	98.88	10	68	22
KB02-2	0.02	21.46	2.45	8.99	37.64	19.50	0.16	9.22	0.05	-	-	99.49	7	54	38
KB03-1	-	22.14	2.86	7.67	36.84	19.44	0.35	9.66	0.05	0.03	0.39	99.43	9	56	36
KB03-2	0.03	13.85	1.74	11.53	36.35	19.81	0.25	15.20	0.02	0.02	-	98.79	5	35	59
KB03-3	-	20.26	2.41	8.66	36.99	19.72	0.33	10.91	0.02	0.04	0.25	99.59	7	51	41
KB03-4	0.06	22.35	2.98	7.46	36.47	19.34	0.47	9.43	-	0.06	0.30	98.89	9	56	34
KB04-1	0.08	27.94	7.30	3.80	36.56	15.46	0.39	6.57	0.04	0.04	0.16	98.33	23	61	16
KB04-2	0.01	28.39	5.20	3.92	37.36	17.42	0.25	6.08	0.01	0.04	0.18	98.86	16	67	17
KB04-3	0.02	23.83	4.88	6.22	36.96	17.47	0.15	9.08	-	0.03		98.65	15	55	30
KB04-4	0.07	28.48	6.20	4.12	36.62	16.65	0.33	5.72	-	0.04	0.34	98.57	19	65	16
KB19-1	0.02	29.82	14.16	3.94	36.38	9.33	0.51	4.88	0.01	-		99.04	49	38	13
KB19-2	-	28.42	4.99	3.24	37.29	17.85	0.43	7.03	0.01	-	0.62	99.88	15	67	18

Cassiterite	CaO (wt %)	FeO (wt %)	Al_2O_3 (wt %)	SnO_2 (wt %)	MnO (wt %)	MgO (wt %)	Nb_2O_5 (wt %)	Ta_2O_5 (wt %)	Total (wt %)
KB02-1	0.27	0.49	-	99.23	-	0.09	0.04	-	100.12
KB12-1	0.30	0.56	-	100.03	0.02	0.10	0.03	0.32	101.37
KB12-2	0.29	0.63	0.02	99.17	-	0.09	0.01	-	100.22
KB30-1	0.25	0.44	-	99.11	-	0.07	0.05	-	99.92
KB30-2	0.18	0.40	0.01	99.50	-	0.07	0.03	-	100.19
KB30-3	0.33	0.52	-	100.01	-	0.11	0.03	-	101.00

Note: "-" means "not detected" or "concentration below detection limits"

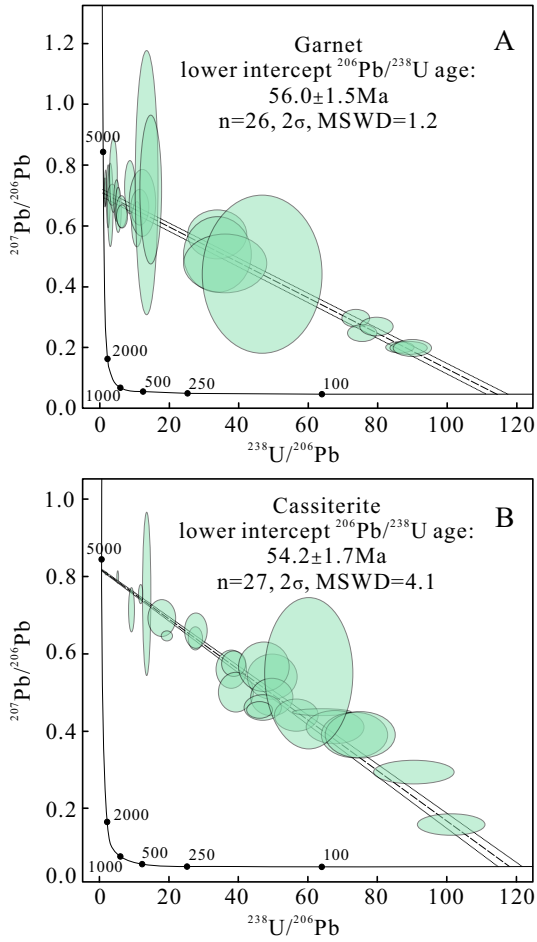

Fig. 4. U-Pb concordia diagrams of garnet (A) and cassiterite (B) from skarns in the Kanbauk deposit, Dawei region, southern Myanmar. MSWD = mean square of weighted deviates.

Ma, respectively (A.L. Pickard, unpub. report, 1996; Jiang et al., 2017).

Our dating results also show that the time span between the early skarn W mineralization from which garnet formed and the late skarn W-Sn mineralization from which cassiterite formed is of the order of several million years. This is in line with most other studies on magmatic-hydrothermal deposits that document ore depositional processes, which typically have an age span from tens to a few hundred thousand years (e.g., Sillitoe and Mortensen, 2010; Chelle-Michou et al., 2015; Zhao et al., 2016; Li et al., 2017), but this relatively short span of time is difficult to define by current in situ U-Pb dating techniques for such old deposits (Chiaradia et al., 2013).

Implications for Regional W-Sn Mineralization

Previous studies have significantly advanced our understanding of the Sn-W mineralization in the Western granitoid province of the Southeast Asian tin belt, but the exact timing of mineralization has been poorly constrained by modern techniques. Although Chhibber (1934) inferred a Late Cretaceous to Eocene range for granites in the Shan Scarps and Tanintharі, the isotopic dating on granites since 1970s has yielded ages scattered from 180 to 20 Ma (Crow and Zaw, 2017, and references therein). Recently, direct dating of hydrothermal

Table 2. Representative LA-ICP-MS U-Pb Dating Results of Garnet and Cassiterite from the Kanbauk Skarns, Dawei Region, Southern Myanmar

Garnet	U (ppm)	$^{207}Pb/^{235}U$ ratio	$^{207}Pb/^{235}U$ (1σ)	$^{206}Pb/^{238}U$ ratio	$^{206}Pb/^{238}U$ (1σ)	Rho	$^{206}Pb/^{238}U$ age (Ma)	$^{206}Pb/^{238}U$ (1σ)
KB04-2	0.18	7.57779	1.06501	0.08130	0.01006	0.88	503.9	59.9
KB04-3	306	0.32067	0.01395	0.01157	0.00022	0.44	74.1	1.4
KB04-4	63.9	0.30815	0.01556	0.01123	0.00028	0.49	72.0	1.8
KB04-11	60.3	0.55331	0.02534	0.01357	0.00031	0.49	86.9	1.9
KB04-13	0.27	19.86357	1.54272	0.21061	0.01396	0.85	1232.1	74.3
KB04-14	0.13	41.67853	4.03933	0.43313	0.03291	0.78	2319.8	148.0
KB04-15	0.08	27.77273	4.24254	0.28628	0.04335	0.99	1622.9	217.3
KB04-16	80.4	0.30462	0.01859	0.01111	0.00027	0.40	71.3	1.8
KB04-17	0.76	11.59912	1.02249	0.11562	0.00851	0.84	705.3	49.2
KB04-18	0.25	17.26618	1.43564	0.19191	0.01332	0.83	1131.7	72.0
KB04-21	0.11	31.57106	3.88934	0.34163	0.03097	0.74	1894.5	148.8
KB04-23	0.43	7.86541	0.64999	0.09392	0.00611	0.79	578.7	36.0
KB04-24	0.37	6.81999	1.10316	0.06872	0.00564	0.51	428.4	34.0
KB04-26	134	0.45258	0.02228	0.01324	0.00030	0.47	84.8	1.9
KB04-31	0.14	14.47013	1.57623	0.16229	0.01685	0.95	969.5	93.4
KB04-32	0.20	13.74802	1.32547	0.15763	0.01473	0.97	943.6	82.1
KB04-35	0.43	1.82335	0.28908	0.02775	0.00375	0.85	176.4	23.5
KB04-37	0.30	7.69114	2.00092	0.07512	0.00771	0.39	466.9	46.2
KB04-41	0.18	66.07433	5.29170	0.67488	0.05047	0.93	3324.7	194.2
KB04-42	0.46	1.30295	0.37113	0.02140	0.00324	0.53	136.5	20.5
KB04-46	0.13	27.05948	3.40443	0.25607	0.02759	0.86	1469.7	141.6
KB04-48	83.4	0.46812	0.02479	0.01257	0.00031	0.47	80.5	2.0
KB04-50	0.45	2.04896	0.31726	0.02942	0.00346	0.76	186.9	21.7
KB04-51	0.66	2.33316	0.27160	0.02962	0.00301	0.87	188.2	18.8
KB04-53	0.20	62.02728	3.85428	0.61913	0.03300	0.86	3106.4	131.4
KB04-54	0.52	7.94252	0.77403	0.08689	0.00785	0.93	537.1	46.6

Cassiterite	U (ppm)	$^{207}Pb/^{235}U$ ratio	$^{207}Pb/^{235}U$ (1σ)	$^{206}Pb/^{238}U$ ratio	$^{206}Pb/^{238}U$ (1σ)	Rho	$^{206}Pb/^{238}U$ age (Ma)	$^{206}Pb/^{238}U$ (1σ)
KB30-2	1,020	10.66473	0.54052	0.10847	0.00427	0.78	663.9	24.8
KB30-4	223	1.49828	0.11068	0.02011	0.00118	0.80	128.4	7.5
KB30-6	1,640	3.19166	0.11093	0.03623	0.00105	0.83	229.4	6.5
KB30-11	110	1.64585	0.13053	0.02111	0.00135	0.81	134.7	8.6
KB30-14	1,080	4.58203	0.16508	0.05149	0.00180	0.97	323.7	11.0
KB30-16	1,340	7.60546	0.90713	0.07306	0.00259	0.30	454.6	15.6
KB30-20	355	1.75168	0.11754	0.02540	0.00132	0.77	161.7	8.3
KB30-22	1,380	0.83360	0.05537	0.01474	0.00074	0.76	94.3	4.7
KB30-23	1,540	1.07378	0.06424	0.01765	0.00080	0.76	112.8	5.1
KB30-26	1,510	0.72019	0.06205	0.01342	0.00078	0.68	85.9	5.0
KB30-28	337	57.88861	1.47751	0.51997	0.01325	0.99	2699.0	56.2
KB30-29	1,600	20.92844	0.35043	0.19000	0.00285	0.90	1121.4	15.4
KB30-30	845	3.27224	0.18323	0.03602	0.00173	0.86	228.1	10.8
KB30-33	473	1.35543	0.08776	0.02017	0.00101	0.78	128.7	6.4
KB30-34	4,150	0.44579	0.02966	0.01104	0.00058	0.79	70.8	3.7
KB30-35	12,000	0.21169	0.01888	0.00988	0.00039	0.44	63.4	2.5
KB30-36	1,470	0.72513	0.05712	0.01351	0.00066	0.62	86.5	4.2
KB30-37	3,440	0.96343	0.05343	0.01560	0.00086	0.99	99.8	5.4
KB30-39	220	5.29463	0.49578	0.05555	0.00496	0.95	348.5	30.3
KB30-40	1,350	2.03218	0.12322	0.02634	0.00127	0.80	167.6	8.0
KB30-42	1,490	1.34723	0.07503	0.02122	0.00100	0.84	135.4	6.3
KB30-43	585	1.66380	0.16873	0.02157	0.00176	0.81	137.6	11.1
KB30-44	1,760	2.04649	0.09090	0.02588	0.00098	0.85	164.7	6.2
KB30-45	3,170	1.36004	0.05245	0.02172	0.00072	0.86	138.5	4.6
KB30-46	728	1.25288	0.21259	0.01656	0.00143	0.51	105.9	9.1
KB30-47	1,040	1.61247	0.12243	0.02157	0.00159	0.97	137.6	10.0
KB30-48	1,340	8.73283	0.24692	0.08393	0.00210	0.88	519.6	12.5

LA-ICP-MS = laser ablation-inductively coupled plasma-mass spectrometry

minerals is available, but only for several primary Sn-W deposits (Fig. 1). In northern Myanmar and adjacent parts of southwest China, the Early Cretaceous Tieyaoshan (123–120 Ma) and Dapingba (120–113 Ma) deposits are thought to be related to the subduction of the Meso-Tethys (Chen et al., 2014; Li et al., 2018). The Late Cretaceous to Paleocene (88–61 Ma) deposits are widely present in the whole Western granitoid province and are related to an Andean-type subduction of the Neo-Tethys since 90 Ma (Mitchell et al., 2012; Gardiner et al., 2016; Jiang et al., 2017; Mao et al., 2020). The ages of the early Eocene Lailishan deposit (52–47 Ma) in Yunnan of southwest China next to northern Myanmar and the Mawchi deposit (42–41 Ma) in central Myanmar were confirmed by cassiterite, molybdenite, and muscovite dating (Chen et

al., 2014; Myint et al., 2018). The direct dating of garnet and cassiterite from Kanbauk skarns yielded the first Eocene age (~55 Ma)—the youngest age of mineral deposits currently revealed in southern Myanmar (Table 3). Accordingly, the Eocene W-Sn mineralization may occur in the whole Western granitoid province from north to south.

In the Dawei region, Eocene granites are identified in the Auk Bok Island west of the Coastal belt, with two zircon U-Pb ages of 52.1 ± 0.6 and 49.7 ± 0.5 Ma (Crow and Zaw, 2017). Some granites in the Coastal belt near Dawei city have zircon U-Pb ages of 62.3 ± 0.6 (Gardiner et al., 2016), 64.1 ± 1.6 (Gardiner et al., 2017), 58.7 ± 0.5, and 60.5 ± 0.8 Ma (Hlaing et al., 2014). For the W-Sn mineralizations in quartz veins in the Kanbauk area, Zhang et al. (2022) acquired a cassiterite U-Pb age of 61.3 ± 0.6 Ma and a wolframite U-Pb age of 62.4 ± 2.4 Ma. Accordingly, the 64 to 50 Ma magmatic event in the Coastal belt is in line with the 62 to 55 Ma skarn and quartz vein mineralizations in the Kanbauk area. In the Central belt, the Thaling Taung, Bawapin, Thitkhatoe, Taungphila, Kalonta, Hermyingyi, and Pagaye deposits have cassiterite and wolframite U-Pb ages of 70 to 60 Ma (Li et al., 2018; Zhang et al., 2022), and the Wagone and Hermyingyi deposits have molybdenite Re-Os ages of 64.5 ± 3.7 and 68.4 ± 2.5 Ma (Jiang et al., 2019; Myint et al., 2021). Four zircon U-Pb ages of granites in the Central belt are reported: 61.7 ± 1.3, 68.8 ± 1.0, 70.0 ± 0.4, and 75.6 ± 8.8 Ma (Crow and Zaw, 2017; Gardiner et al., 2017; Jiang et al., 2017). In the Frontier belt, Charusiri (1989) obtained muscovite Ar-Ar ages of 76.5 to 74.4 Ma for the Pilok deposit and a biotite Ar-Ar age of 72 Ma for the granite 8 km northwest of the Pilok deposit. As summarized in Table 3, we can identify a younging trend of mineralization from the Frontier belt (77–74 Ma), to the Central belt (70–60 Ma), to the Coastal belt (62–55 Ma), which is also in line with the trend of the published granite ages in this region (Fig. 5). The younging trends from east to west are also expressed in Yunnan next to northern Myanmar, where the eastern Xiaolonghe deposit is 74 to 72 Ma and the western Lailishan deposit is 52 to 47 Ma (Chen et al., 2014). In central Myanmar, the Pyiyadana, Tagung Taung, and Shwechung deposits in the northern Padatgyaung region are 69 to 61 Ma (Myint et al., 2021), and the southern Marchi deposit is ~43 Ma (Myint et al., 2018). Because the ancient continental margin was proposed to be westward facing but eastward convex (Mitchell and Garson, 1981), the Mawchi deposit was likely much closer to the margin than those deposits in the Padatgyaung region. Therefore, the younging trend of W-Sn mineralization to the west during the Late Cretaceous to early Eocene identified in the Dawei region may extend to the whole Western granitoid province.

Tungsten and Sn mineralization is generally considered to be related to metasedimentary-derived S-type granites, such as those in the Erzgebirge in Europe or Main Range Malaysia (e.g., Ng et al., 2015; Romer and Kroner, 2015). However, in the Western granitoid province of Southeast Asian tin belt, more and more granites related to W-Sn mineralization are recently identified to be distinctively A_2 type, including the Hermyingyi and Taungphila granites in southern Myanmar (Jiang et al., 2017), the Xiaolonghe and Dasongpo granites in Yunnan next to northern Myanmar (Chen et al., 2015), and the Mawchi granite in central Myanmar (Myint et al., 2017).

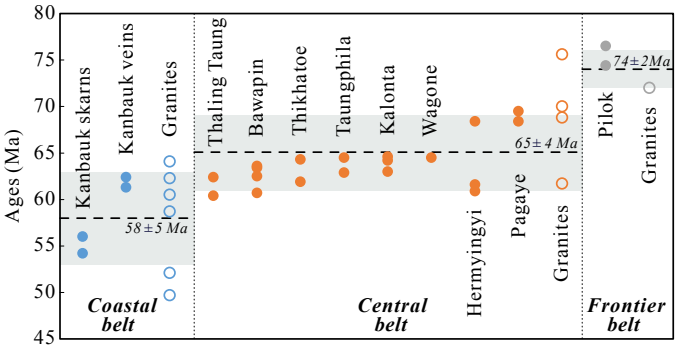

Fig. 5. Plots of published ages of W-Sn deposits and granites in the Dawei region, southern Myanmar. The dashed lines are the average ages of mineralization and granites in each belt, and the gray areas show the age errors.

The A_2-type granites are considered to be derived from continental crust that had been through a cycle of continent-continent collision or processed through a subduction zone and are emplaced in extensional tectonic environments (Eby, 1992). During the Late Cretaceous to early Eocene, an E-dipping subduction zone was developed on the margin of Neo-Tethys, where the arc magmatism is proximal to the subduction zone and the granite belt is distal to the subduction zone, and possible E-directed thrusts are in a zone east of the tin granites, supporting a prolonged Andean-type magmatic-arc system (Mitchell and Garson, 1981; Gardiner et al., 2015). Since the Late Cretaceous, a proposed slab rollback of Neo-Tethys, as suggested by the increase of the convergence rate, could have induced a back-arc extensional zone (Wen et al., 2008; Jiang et al., 2017; Mitchell, 2018). In the back-arc area, relaxation of compressive stress would have allowed the rise of the thickened crust and tectonic erosion, and underplating of the mantle-derived magma provided heat for crust melting (Jiang et al., 2017; Mitchell, 2018). In this scenario, the mineralized granites in the Western granitoid province were generated from the partial melting of the fertile Paleoproterozoic continental crust and underwent strong differentiation and gradual enrichment in Sn and W (Chen et al., 2015; Romer and Kroner, 2015, 2016; Jiang et al., 2017; Myint et al., 2017). On a regional scale, carbonate sedimentary rocks favored the development of replacement skarn W-Sn deposits, where brittle clastic rocks host quartz-vein W-Sn deposits.

The newly defined younging trend of mineralization toward the west in the Western granitoid province of the Southeast Asian tin belt provides further support to the postulated westward rollback of Neo-Tethyan oceanic slab and trench retreat, which are considered as the main mechanisms for the regional, extensive Sn-W mineralization (e.g., Jiang et al., 2017; Mitchell, 2018). However, detailed studies regarding the classification and age of granites in this belt will be required in the future to better understand the regional metallogeny.

Conclusions

The recently identified Kanbauk skarn W-Sn(-F) deposit was formed during the early Eocene, as constrained by U-Pb ages of garnet and cassiterite. The newly obtained age is the first reported age of hydrothermal minerals of the Kanbauk skarns and is significantly younger than those of regional quartz-vein-

Table 3. Summary of Published Direct Dating Results of Hydrothermal Minerals from W-Sn Deposits in the Western Granitoid Province and Published Ages of Granites in the Dawei Region, Southern Myanmar

Districts		Deposits	Sampling	Methods	Age (Ma)	References
Northern Myanmar and adjacent parts of SW China						
		Lailishan Sn	Quartz vein	Cassiterite U-Pb	47.4 ± 2.0	Chen et al. (2014)
				Muscovite Ar-Ar	48.4 ± 0.3	
			Greisen	Cassiterite U-Pb	52.0 ± 2.7	
		Xiaolonghe Sn	Quartz vein and greisen	Cassiterite U-Pb	71.9 ± 2.3	Chen et al. (2014)
				Muscovite Ar-Ar	71.9 ± 1.4	
		Dapingba Mo-W	Quartz vein	Molybdenite Re-Os	112.8 ± 1.0 to 119.6 ± 1.3	Li et al. (2018)
		Tieyaoshan Sn	Greisen ore	Cassiterite U-Pb	119.3 ± 1.7	Chen et al. (2014)
				Muscovite Ar-Ar	122.4 ± 0.7	
Central Myanmar						
		Mawchi Sn-W	Quartz vein	Muscovite Ar-Ar	40.8 ± 0.1	Myint et al. (2018)
				Molybdenite Re-Os	42.4 ± 1.2	
		Tagung Taung W-Sn	Quartz vein	Molybdenite Re-Os	60.5 ± 0.5	Myint et al. (2021)
		Shwechaung W-Mo	Quartz vein	Molybdenite Re-Os	64.2 ± 0.5	Myint et al. (2021)
		Pyiyadana Sn-W	Greisen	Molybdenite Re-Os	68.5 ± 2.7	Myint et al. (2021)
Southern Myanmar						
Dawei region	Coastal belt	Kanbauk W-Sn	Skarn	Garnet U-Pb	56.0 ± 1.5	This study
				Cassiterite U-Pb	54.2 ± 1.7	
			Quartz vein	Cassiterite U-Pb	61.3 ± 0.6	Zhang et al. (2022)
				Wolframite U-Pb	62.4 ± 2.4	
			Auk Bok granite	Zircon U-Pb	49.7 ± 0.5	A.L. Pickard (unpub. report, 1996)
					52.1 ± 0.6	
			Porphyritic biotite granite	Zircon U-Pb	58.7 ± 0.5	Hlaing et al. (2014)
			Biotite granite	Zircon U-Pb	60.5 ± 0.8	
			Biotite + plagioclase + K-feldspar granite	Zircon U-Pb	62.3 ± 0.6	Gardiner et al. (2016)
			Biotite + plagioclase + K-feldspar granite	Zircon U-Pb	64.1 ± 1.6	Gardiner et al. (2017)
	Central belt	Thaling Taung Sn-W	Quartz vein	Cassiterite U-Pb	60.4 ± 0.9	Zhang et al. (2022)
				Wolframite U-Pb	62.4 ± 0.8	
		Bawapin Sn-W	Quartz vein	Cassiterite U-Pb	60.7 ± 2.5	Li et al. (2018)
			Nearby mineralized granite	Cassiterite U-Pb	62.5 ± 1.0	
			Quartz vein	Cassiterite U-Pb	63.6 ± 0.6	Zhang et al. (2022)
				Wolframite U-Pb	63.4 ± 0.8	
		Thitkhatoe Sn-W	Quartz vein	Cassiterite U-Pb	61.9 ± 0.6	Zhang et al. (2022)
				Wolframite U-Pb	64.3 ± 2.9	
		Taungphila Sn-W	Quartz vein and greisen	Cassiterite U-Pb	62.9 ± 0.6	Zhang et al. (2022)
				Wolframite U-Pb	64.5 ± 1.1	
		Kalonta Sn-W	Quartz vein	Cassiterite U-Pb	63.0 ± 0.6	Zhang et al. (2022)
				Wolframite U-Pb	64.2 ± 2.2	
				Cassiterite U-Pb	64.6 ± 3.9	Li et al. (2018)
		Wagone W-Sn-Mo	Quartz vein	Molybdenite Re-Os	64.5 ± 3.7	Myint et al. (2021)
		Hermyingyi W-Sn	Quartz vein	Cassiterite U-Pb	61.6 ± 0.8	Zhang et al. (2022)
				Wolframite U-Pb	60.9 ± 1.3	
				Molybdenite Re-Os	68.4 ± 2.5	Jiang et al. (2019)
		Pagaye Sn-W	Quartz vein	Cassiterite U-Pb	69.5 ± 0.5	Zhang et al. (2022)
				Wolframite U-Pb	68.4 ± 2.7	
			Hermyingyi granite	Zircon U-Pb	61.7 ± 1.3	A.L. Pickard (unpub. report, 1996)
				Zircon U-Pb	70.0 ± 0.4	Jiang et al. (2017)
			Taungphila monzogranite	Zircon U-Pb	68.8 ± 1.0	Jiang et al. (2017)
			Biotite + plagioclase + K-feldspar granite	Zircon U-Pb	75.6 ± 8.8	Gardiner et al. (2017)
	Frontier belt	Pilok Sn-W	Quartz vein	Muscovite Ar-Ar	74.4 to 76.5	Charusiri (1989)
			Biotite granite	Biotite Ar-Ar	72	Charusiri (1989)
Outside Dawei region		Letha Taung Sn-W	Quartz vein	Cassiterite U-Pb	84.9 ± 0.5	Zhang et al. (2022)
				Wolframite U-Pb	85.2 ± 2.2	
		Kuntabin Sn-W	Quartz vein	Cassiterite U-Pb	88.1 ± 1.9	Mao et al. (2020)
			Quartz vein and greisen	Molybdenite Re-Os	87.7 ± 0.5	

type W-Sn mineralization, implying separate mineralizing events in the Kanbauk area. By integrating previously published dates of primary Sn-W deposits in the Dawei region with dates from this study, we recognize for the first time the younging trend of mineralization toward the west coastal areas and provide support for the rollback of the Neo-Tethyan subducting slab since the Late Cretaceous. The postulated slab rollback can be considered as the main mechanism for the regional, extensive Sn-W mineralization.

Acknowledgments

This study is financially supported by the National Science Foundation of China (42102090) and Fundamental Research Funds for the Central Universities, China University of Geosciences (Wuhan) (CUG2106104). We thank Kevin Flaherty and Savitar's Kanbauk camp crews for their field support in the past years. We are also grateful to Khin Zaw, Kuidong Zhao, Xiaoran Zhang, Xiao Fu, Tao Luo, Yanwen Tang, and Junjie Han for their initial discussions and technical support. This manuscript was significantly improved with constructive reviews by Editor Larry Meinert, Douglas Kirwin, Martin Palmer, and an anonymous referee.

REFERENCES

Charusiri, P., 1989, Lithophile metallogenetic epochs of Thailand: A geological and geochronological investigation: Ph.D. thesis, Kingston, London, Queen's University, 809 p.

Chelle-Michou, C., Chiaradia, M., Selby, D., Ovtcharova, M., and Spikings, R.A., 2015, High-resolution geochronology of the Coroccohuayco porphyry-skarn deposit, Peru: A rapid product of the Incaic orogeny: Economic Geology, v. 110, p. 423–443.

Chen, X.-C., Hu, R.-Z., Bi, X.-W., Li, H.-M., Lan, J.-B., Zhao, C.-H., and Zhu, J.-J., 2014, Cassiterite LA-MC-ICP-MS U/Pb and muscovite $^{40}Ar/^{39}Ar$ dating of tin deposits in the Tengchong-Lianghe tin district, NW Yunnan, China: Mineralium Deposita, v. 49, no. 7, p. 843–860.

Chen, X.-C., Hu, R.-Z., Bi, X.-W., Zhong, H., Lan, J.-B., Zhao, C.-H., and Zhu, J.-J., 2015, Petrogenesis of metaluminous A-type granitoids in the Tengchong-Lianghe tin belt of southwestern China: Evidences from zircon U-Pb ages and Hf-O isotopes, and whole-rock Sr-Nd isotopes: Lithos, v. 212, p. 93–110.

Chhibber, H.L., 1934, The geology of Burma: London, Macmillan, 538 p.

Chiaradia, M., Schaltegger, U., Spikings, R., Wotzlaw, J.F., and Ovtcharova, M., 2013, How accurately can we date the duration of magmatic-hydrothermal events in porphyry systems?—an invited paper: Economic Geology, v. 108, no. 4, p. 565–584.

Clegg, E.L.G., 1994, The mineral deposits of Burma: Bombay, Times of India Press, 38 p.

Cobbing, E., Mallick, D., Pitfield, P., and Teoh, L., 1986, The granites of the Southeast Asian tin belt: Journal of the Geological Society, London, v. 143, no. 3, p. 537–550.

Coggin Brown, J., and Heron, A., 1923, The geology and ore deposits of the Tavoy district: Memoirs of the Geological Survey of India, v. 44, part 2, p. 167–354.

Crow, M.J., and Zaw, K., 2017, Geochronology in Myanmar (1964–2017): Geological Society, London, Memoir 48, p. 713–759.

Deng, X.-D., Li, J.-W., Luo, T., and Wang, H.-Q., 2017, Dating magmatic and hydrothermal processes using andradite-rich garnet U-Pb geochronometry: Contributions to Mineralogy and Petrology, v. 172, no. 9, article 71, doi: 10.1007/s00410-017-1389-2.

Eby, G.N., 1992, Chemical subdivision of the A-type granitoids: Petrogenetic and tectonic implications: Geology, v. 20, no. 7, p. 641–644.

Gardiner, N.J., Searle, M.P., Robb, L.J., and Morley, C.K., 2015, Neo-Tethyan magmatism and metallogeny in Myanmar—an Andean analogue?: Journal of Asian Earth Sciences, v. 106, p. 197–215.

Gardiner, N.J., Robb, L.J., Morley, C.K., Searle, M.P., Cawood, P.A., Whitehouse, M.J., Kirkland, C.L., Roberts, N.M., and Myint, T.A., 2016, The tectonic and metallogenic framework of Myanmar: A Tethyan mineral system: Ore Geology Reviews, v. 79, p. 26–45.

Gardiner, N.J., Hawkesworth, C.J., Robb, L.J., Whitehouse, M.J., Roberts, N.M.W., Kirkland, C.L., and Evans, N.J., 2017, Contrasting granite metallogeny through the zircon record: A case study from Myanmar: Scientific Reports, v. 7, no. 1, article 748.

Griffiths, H.D., 1917, The Kanbauk wolfram mine: The Mining Magazine, v. 17, p. 211–219.

Gulson, B.L., and Jones, M.T., 1992, Cassiterite: Potential for direct dating of mineral deposits and a precise age for the Bushveld Complex granites: Geology, v. 20, no 4, p. 355–358.

Hlaing, S.S., Sanematsu, K., Manaka, T., Hla, K., and Thein, W., 2014, Geochemical characteristics of the granitoid rocks from Tawmore Taung area, Launglon township, Tanintharyi region, Myanmar: Myanmar Geosciences Society, GEOSEA XIII–GeoMyanmar, Yangon, Mayanmar, March 10–11, 2014, Poster Presentation 3.

Hu, Z., Zhang, W., Liu, Y., Gao, S., Li, M., Zong, K., Chen, H., and Hu, S., 2014, "Wave" signal-smoothing and mercury-removing device for laser ablation quadrupole and multiple collector ICPMS analysis: Application to lead isotope analysis: Analytical Chemistry, v. 87, p. 1152–1157.

Hutchison, C., and Taylor, D., 1978, Metallogenesis in SE Asia: Journal of the Geological Society, London, v. 135, no. 4, p. 407–428.

Jiang, H., Li, W.-Q., Jiang, S.-Y., Wang, H., and Wei, X.-P., 2017, Geochronological, geochemical and Sr-Nd-Hf isotopic constraints on the petrogenesis of Late Cretaceous A-type granites from the Sibumasu block, southern Myanmar, SE Asia: Lithos, v. 268, p. 32–47.

Jiang, H., Jiang, S.-Y., Li, W., and Zhao, K., 2019, Timing and source of the Hermyingyi W-Sn deposit in southern Myanmar, SE Asia: Evidence from molybdenite Re-Os age and sulfur isotopic composition: Journal of Earth Science, v. 30, no. 1, p. 70–79.

Lehmann, B., 2021, Formation of tin ore deposits: A reassessment: Lithos, v. 402–403, article 105756.

Lehmann, B., Jungyusuk, N., Khositanont, S., Höhndorf, A., and Kuroda, Y., 1994, The tin-tungsten ore system of Pilok, Thailand: Journal of Southeast Asian Earth Sciences, v. 10, no. 1, p. 51–63.

Li, J.-X., Zhang, L.-Y., Fan, W.-M., Ding, L., Sun, Y.-L., Peng, T.-P., Li, G.-M., and Sein, K., 2018, Mesozoic-Cenozoic tectonic evolution and metallogeny in Myanmar: Evidence from zircon/cassiterite U-Pb and molybdenite Re-Os geochronology: Ore Geology Reviews, v. 102, p. 829–845.

Li, Y., Selby, D., Condon, D., and Tapster, S., 2017, Cyclic magmatic-hydrothermal evolution in porphyry systems: High-precision U-Pb and Re-Os geochronology constraints on the Tibetan Qulong porphyry Cu-Mo deposit: Economic Geology, v. 112, no. 6, p. 1419–1440.

Liu, L., Hu, R.-Z., Zhong, H., Yang, J.-H., Kang, L.-F., Zhang, X.-C., Fu, Y.-Z., Mao, W., and Tang, Y.-W., 2020, Petrogenesis of multistage S-type granites from the Malay Peninsula in the Southeast Asian tin belt and their relationship to Tethyan evolution: Gondwana Research, v. 84, p. 20–37.

Liu, Y., Hu, Z., Zong, K., Gao, C., Gao, S., Xu, J., and Chen, H., 2010, Reappraisement and refinement of zircon U-Pb isotope and trace element analyses by LA-ICP-MS: Chinese Science Bulletin, v. 55, no. 15, p. 1535–1546.

Luo, T., Hu, Z., Zhang, W., Günther, D., Liu, Y., Zong, K., and Hu, S., 2018a, Reassessment of the influence of carrier gases He and Ar on signal intensities in 193 nm excimer LA-ICP-MS analysis: Journal of Analytical Atomic Spectrometry, v. 33, no. 10, p. 1655–1663.

Luo, T., Hu, Z., Zhang, W., Liu, Y., Zong, K., Zhou, L., Zhang, J., and Hu, S., 2018b, Water vapor-assisted "universal" nonmatrix-matched analytical method for the in situ U-Pb dating of zircon, monazite, titanite, and xenotime by laser ablation-inductively coupled plasma mass spectrometry: Analytical Chemistry, v. 90, no. 15, p. 9016–9024.

Mao, W., Zhong, H., Yang, J., Tang, Y., Liu, L., Fu, Y., Zhang, X., Sein, K., Aung, S.M., Li, J., and Zhang, L., 2020, Combined zircon, molybdenite, and cassiterite geochronology and cassiterite geochemistry of the Kuntabin tin-tungsten deposit in Myanmar: Economic Geology, v. 115, no. 3, p. 603–625.

Meinert, L.D., 1992, Skarns and skarn deposits: Geoscience Canada, v. 19, no. 4, p. 145–162.

Metcalfe, I., 2002, Permian tectonic framework and palaeogeography of SE Asia: Journal of Asian Earth Sciences, v. 20, no. 6, p. 551–566.

Mezger, K., Hanson, G.N., and Bohlen, S.R., 1989, U-Pb systematics of garnet—dating the growth of garnet in the late Archean Pikwitonei granulite domain at Cauchon and Natawahunan lakes, Manitoba, Canada: Contributions to Mineralogy and Petrology, v. 101, no. 2, p. 136–148.

Mitchell, A., 1977, Tectonic settings for emplacement of Southeast Asian tin granites: Geological Society of Malaysia Bulletin, v. 9, p. 123–140.

——2018, Geological belts, plate boundaries, and mineral deposits in Myanmar: Elsevier, 509 p.

Mitchell, A., Chung, S.-L., Oo, T., Lin, T.-H., and Hung, C.-H., 2012, Zircon U-Pb ages in Myanmar: Magmatic-metamorphic events and the closure of a Neo-Tethys ocean?: Journal of Asian Earth Sciences, v. 56, p. 1–23.

Mitchell, A.H.G., and Garson, M.S., 1981, Mineral deposits and global tectonic settings: Academic Press, 405 p.

Myint, A.Z., Zaw, K., Swe, Y.M., Yonezu, K., Cai, Y., Manaka, T., and Watanabe, K., 2017, Geochemistry and geochronology of granites hosting the Mawchi Sn-W deposit, Myanmar: Implications for tectonic setting and emplacement: Geological Society of London, Memoir 48, p. 385–400.

Myint, A.Z., Yonezu, K., Boyce, A.J., Selby, D., Scherstén, A., Tindell, T., Watanabe, K., and Swe, Y.M., 2018, Stable isotope and geochronological study of the Mawchi Sn-W deposit, Myanmar: Implications for timing of mineralization and ore genesis: Ore Geology Reviews, v. 95, p. 663–679.

Myint, A.Z., Li, H., Mitchell, A., Selby, D., and Wagner, T., 2021, Geology, mineralogy, ore paragenesis, and molybdenite Re-Os geochronology of Sn-W(-Mo) mineralization in Padatgyaung and Dawei, Myanmar: Implications for timing of mineralization and tectonic setting: Journal of Asian Earth Sciences, v. 212, article 104725.

Ng, S., Whitehouse, M., Searle, M., Robb, L., Ghani, A., Chung, S., Oliver, G., Sone, M., Gardiner, N., and Roselee, M., 2015, Petrogenesis of Malaysian tin granites: Part 1. Geochemistry and fractional crystallization of the Malaysian tin granites: Geological Society of America Bulletin, v. 127, no. 9–10, p. 1209–1237.

Ridd, M.F., and Watkinson, I., 2013, The Phuket-Slate belt terrane: Tectonic evolution and strike-slip emplacement of a major terrane on the Sundaland margin of Thailand and Myanmar: Proceedings of the Geologists' Association, v. 124, no. 6, p. 994–1010.

Romer, R.L., and Kroner, U., 2015, Sediment and weathering control on the distribution of Paleozoic magmatic tin-tungsten mineralization: Mineralium Deposita, v. 50, no. 3, p. 327–338.

——2016, Phanerozoic tin and tungsten mineralization—tectonic controls on the distribution of enriched protoliths and heat sources for crustal melting: Gondwana Research, v. 31, p. 60–95.

Schwartz, M., Rajah, S., Askury, A., Putthapiban, P., and Djaswadi, S., 1995, The southeast Asian tin belt: Earth-Science Reviews, v. 38, no. 2, p. 95–293.

Schwartz, M.O., and Askury, A., 1990, Granite magmatism and tin-tungsten metallogenesis in the Kuantan-Dungun area, Malaysia: Geological Society of Malaysia Bulletin, v. 26, p. 147–179.

Searle, M., Whitehouse, M., Robb, L., Ghani, A., Hutchison, C., Sone, M., Ng, S.-P., Roselee, M., Chung, S.-L., and Oliver, G., 2012, Tectonic evolution of the Sibumasu-Indochina terrane collision zone in Thailand and Malaysia: Constraints from new U-Pb zircon chronology of SE Asian tin granitoids: Journal of the Geological Society, London, v. 169, no. 4, p. 489–500.

Searle, M.P., Robb, L.J., and Gardiner, N.J., 2016, Tectonic processes and metallogeny along the Tethyan mountain ranges of the Middle East and South Asia (Oman, Himalaya, Karakoram, Tibet, Myanmar, Thailand, Malaysia): Society of Economic Geologists, Special Publication 19, p. 301–327.

Seman, S., Stockli, D.F., and McLean, N., 2017, U-Pb geochronology of grossular-andradite garnet: Chemical Geology, v. 460, p. 106–116.

Sillitoe, R.H., and Mortensen, J.K., 2010, Longevity of porphyry copper formation at Quellaveco, Peru: Economic Geology, v. 105, no. 6, p. 1157–1162.

Stauffer, P.H., and Lee, C.P., 1986, Late Palaeozoic glacial marine facies in Southeast Asia and its implications: Geological Society of Malaysia Bulletin, v. 20, p. 363–397.

Tang, Y., Gao, J., Lan, T., Cui, K., Han, J., Zhang, X., Chen, Y., and Chen, Y., 2021, In situ low-U garnet U-Pb dating by LA-SF-ICP-MS and its application in constraining the origin of Anji skarn system combined with Ar-Ar dating and Pb isotopes: Ore Geology Reviews, v. 130, article 103970.

Vermeesch, P., 2018, IsoplotR: A free and open toolbox for geochronology: Geoscience Frontiers, v. 9, no. 5, p. 1479–1493.

Wen, D.-R., Liu, D., Chung, S.-L., Chu, M.-F., Ji, J., Zhang, Q., Song, B., Lee, T.-Y., Yeh, M.-W., and Lo, C.-H., 2008, Zircon SHRIMP U-Pb ages of the Gangdese batholith and implications for Neotethyan subduction in southern Tibet: Chemical Geology, v. 252, no. 3, p. 191–201.

Yang, J.-H., Zhou, M.-F., Hu, R.-Z., Zhong, H., Williams-Jones, A.E., Liu, L., Zhang, X.-C., Fu, Y.-Z., and Mao, W., 2020, Granite-related tin metallogenic events and key controlling factors in peninsular Malaysia, Southeast Asia: New insights from cassiterite U-Pb dating and zircon geochemistry: Economic Geology, v. 115, no. 3, p. 581–601.

Yuan, S., Peng, J., Hao, S., Li, H., Geng, J., and Zhang, D., 2011, In situ LA-MC-ICP-MS and ID-TIMS U-Pb geochronology of cassiterite in the giant Furong tin deposit, Hunan province, South China: New constraints on the timing of tin-polymetallic mineralization: Ore Geology Reviews, v. 43, no. 1, p. 235–242.

Zaw, K., Meffre, S., Lai, C.-K., Burrett, C., Santosh, M., Graham, I., Manaka, T., Salam, A., Kamvong, T., and Cromie, P., 2014, Tectonics and metallogeny of mainland Southeast Asia—a review and contribution: Gondwana Research, v. 26, no. 1, p. 5–30.

Zhang, Q., Zhao, K.-D., Li, W.-Q., Palmer, M.R., Jiang, S.-Y., Jiang, H., Zhang, W., Zhang, D., and Hussain, A., 2022, Timing and tectonic setting of tin mineralization in southern Myanmar: Constraints from cassiterite and wolframite U-Pb ages: Mineralium Deposita, v. 57, p. 977–999.

Zhao, W.W., Zhou, M.-F., and Chen, W.T., 2016, Growth of hydrothermal baddeleyite and zircon in different stages of skarnization: American Mineralogist, v. 101, no. 12, p. 2689–2700.

Wen Winston Zhao is an associate professor at China University of Geosciences (CUG), Wuhan. He obtained his B.Sc. degree in geology from CUG Wuhan in 2012 and his Ph.D. degree in economic geology from Hong Kong University in 2017. Before joining CUG Wuhan, he worked for three years in Hong Kong as postdoctoral fellow and in Southeast Asia as senior geologist. He is now working on rare metal and rare earth deposits mainly in Southeast Asia and South China.